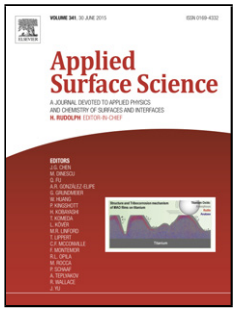

Title: Deposition of carbon nanotubes onto aramid fibers using as-received and chemically modified fibers

Author: O. Rodríguez-Uicab F. Avilés P.I Gonzalez-Chi G. Canché-Escamilla S. Duarte-Aranda M. Yazdani-Pedram P. Toro F. Gamboa M.A. Mazo A. Nistal J. Rubio

PII: S0169-4332(16)31045-5
DOI: http://dx.doi.org/doi:10.1016/j.apsusc.2016.05.037
Reference: APSUSC 33230

To appear in: *APSUSC*

Received date: 9-4-2016
Revised date: 5-5-2016
Accepted date: 6-5-2016

Please cite this article as: O.Rodríguez-Uicab, F.Avilés, P.I Gonzalez-Chi, G.Canché-Escamilla, S.Duarte-Aranda, M.Yazdani-Pedram, P.Toro, F.Gamboa, M.A.Mazo, A.Nistal, J.Rubio, Deposition of carbon nanotubes onto aramid fibers using as-received and chemically modified fibers, Applied Surface Science http://dx.doi.org/10.1016/j.apsusc.2016.05.037

Deposition of carbon nanotubes onto aramid fibers using as-received and chemically modified fibers

O. Rodríguez-Uicab[a], F. Avilés[a,*], P.I Gonzalez-Chi[a], G. Canché-Escamilla[a], S. Duarte-Aranda[a], M. Yazdani-Pedram[b], P. Toro[c], F. Gamboa[d], M.A. Mazo[e], A. Nistal[e], J. Rubio[e]

[a] Centro de Investigación Científica de Yucatán A.C., Unidad de Materiales, Calle 43 No.130, Col. Chuburna de Hidalgo. C.P. 97200, Mérida, Yucatán, Mexico.
[b] Facultad de Ciencias Químicas y Farmacéuticas, Universidad de Chile, S. Livingstone 1007, Independencia, Santiago, Chile.
[c] Facultad de Ciencias Físicas y Matemáticas, Universidad de Chile, Av. Beauchef 850, Santiago, Chile.
[d] Centro de Investigacion y de Estudios Avanzados del IPN, Unidad Mérida, Depto. de Física Aplicada, Km. 6 Antigua Carretera a Progreso, 97310 Mérida, Yucatán, Mexico
[e] Instituto de Cerámica y Vidrio (ICV-CSIC), Kelsen 5, 28049 Madrid, Spain

Graphical abstract

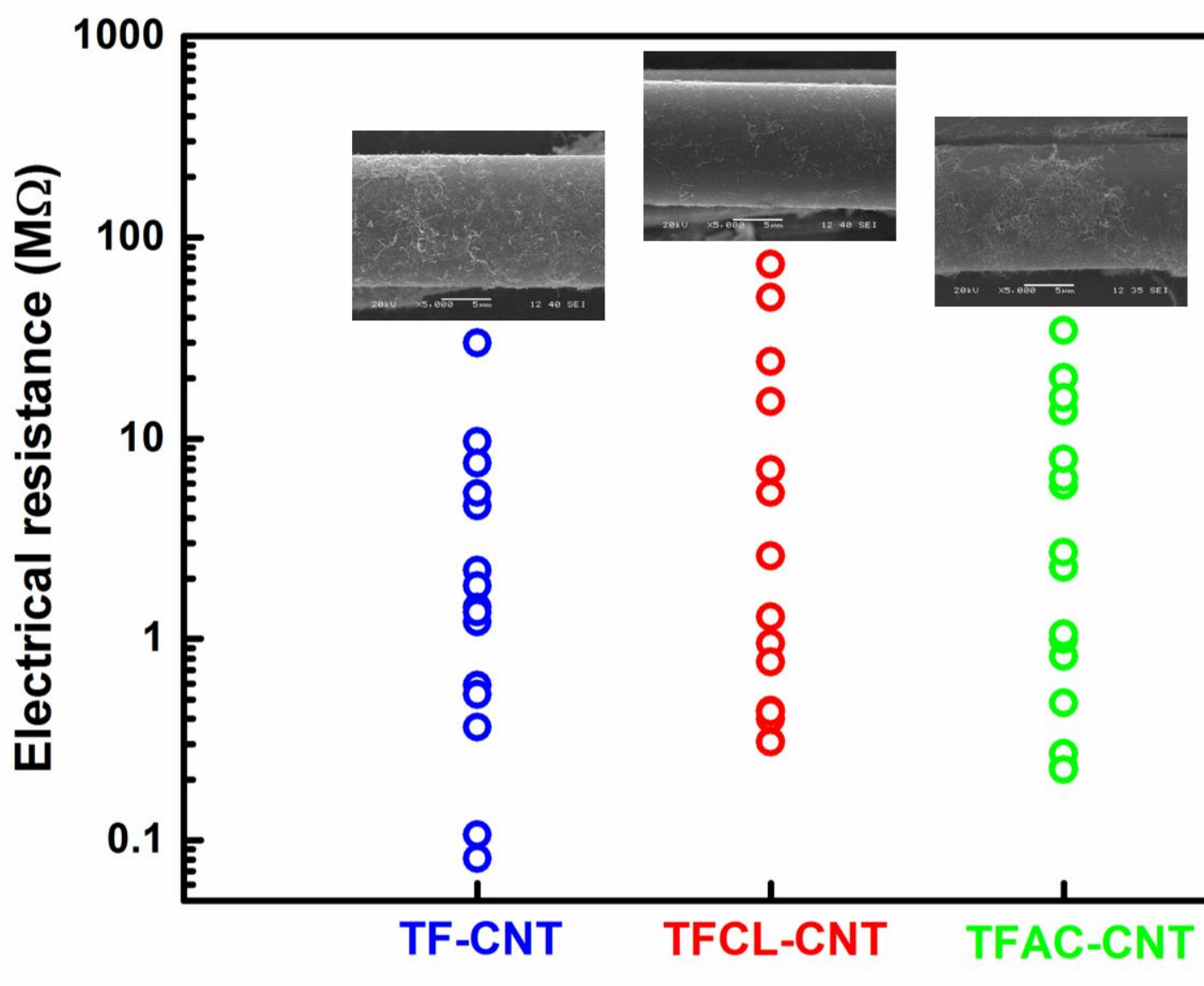

Highlights

- The surface of aramid fibers was functionalized by two acid treatments.
- The treatment based on HNO_3/H_2SO_4 reduced the mechanical properties of the fibers.
- CNTs were deposited on the aramid fibers, reaching electrical conductivity.
- Homogeneous CNT distribution was achieved by using pristine fibers or chlorosulfonic acid.

Abstract

Multiwall carbon nanotubes (MWCNTs) oxidized by an acid treatment were deposited on the surface of as-received comercial aramid fibers containing a surface coating ("sizing"), and fibers modified by either a chlorosulfonic treatment or a mixture of nitric and sulfuric acids. The surface of the aramid fiber activated by the chemical treatments presents increasing density of CO, COOH and OH functional groups. However, these chemical treatments reduced the tensile mechanical properties of the fibers, especially when the nitric and sulfuric acid mixture was used. Characterization of the MWCNTs deposited on the fiber surface was conducted by scanning electron microscopy, Raman spectroscopy mapping and X-ray photoelectron spectroscopy. These characterizations showed higher areal concentration and more homogeneous distribution of MWCNTs over the aramid fibers for as-received fibers and for those modified with chlorosulfonic acid, suggesting the existence of interaction between the oxidized MWCNTs and the fiber coating. The electrical resistance of the MWCNT-modified aramid yarns comprissing ~1000 indivual fibers was in the order of MΩ/cm, which renders multifuncional properties.

Keywords: Aramid fiber, carbon nanotubes, surface treatment, mechanical properties, electrical properties, multifunctional.

*Corresponding author: E-mail address: faviles@cicy.mx (Francis Avilés)

1. Introduction

Aramid fibers are well known for their use in ballistic scenarios and in advanced composites for impact-related applications, such as bulletproof vests, helmets, and high performance composites for transportation and the automobile industry [1, 2]. These fibers do not show a melting point and their thermal descomposition occurs near 400 °C [2-4]. The aromatic rings present in the backbone of the fiber molecular structure promote high thermal stability [5]. Aramid fibers comprise a highly ordered arrangement of polymer chains yielding a rather smooth surface with reduced reactivity [3-7], high crystallinity (~76-95 %) and high mechanical strength [8,9]. However, in the composites materials field, surface modifications of the aramid fibers are often

necessary to activate their surface. There are several surface treatments that have been attempted to promote the generation of functional groups on the surface of aramind fibers, including plasma treatments [10], acid chemical treatments [11] and fluorinations [12]. Wu *et al.* [13], for example, investigated the efect of fiber surface treatments using plasmas of ammonia, oxygen and water vapor, as well as a solution of chlorosulfonic acid in dichloromethane. According to their results, the chlorosulfonic acid treatment produced more changes to the fiber surface morphology than the plasma treatments. Maity *et al.* [14] reported a modification of aramid fibers using fluorination; the C-H bonds of the aromatic rings were substituted by C-F bonds, yielding higher thermal stability. In multiscale hierarchical composites comprising a macro-scale matrix, a fiber with diameter at the micro-scale, and a nanostructure, these kind of surface modifications may improve the interactions not only between the fiber and matrix, but also with the nanostructures deposited onto the fiber surface, such as carbon nanotubes. The current interest in multiscale hierarchical composites focuses on their multifunctionality, and in the case of multiwall carbon nanotubes (MWCNTs) their high electrical conductivity is frequently exploited. MWCNTs have been deposited onto glass and carbon fibers by electrophoretic methods [15, 16] and by simpler methods such as dipping or immersion in nanotube dispersions [17-19]. It has been shown that the deposition of MWCNTs onto engeneering fibers can increase the fiber/matrix interfacial shear strength [20] and delay the onset of microcrack propagation [21]. Furthermore, the generation of a percolative electrical networks on the fiber surface renders composite materials with multifunctional features such as self-sensing of strain and damage [20]. However, research concerning deposition of MWCNTs onto aramid fibers is scarce. O'Connor *et al.* [22] reported the deposition of MWCNTs onto aramid fibers using N-methylpyrrolidone (NMP). The aramid fibers and the MWCNTs were immersed in NMP to swell the fibers, promoting physical interactions between the aramid fibers and the MWCNTs. A similar work was reported by Chen *et al.* [3], where the aramid fibers were modified by a mixture of hexamethylene diisocyanate and 1,4-diazabi-cyclo octane. The MWCNTs were dispersed in NMP and the aramid fibers were inmersed in the MWCNT/NMP solution, promoting fiber swelling and chemical grafting. Given this background and motivation, MWCNTs were herein deposited onto the surface of Twaron fibers using an immersion process assisted by ultrasound; the role of the surface coating of the Twaron fibers was studied examining the effect of two fiber chemical treatments.

2. Materials and methods

2.1. Materials

The aramid fibers used were Twaron 2200 from Teijin Aramid Inc. (Georgia, USA). According to the manufacturer, the fibers have a tensile elastic modulus between 130 and 180 GPa, a density of 1.45 g/cm^3 and individual fiber diameter of ~ 12 µm. The fiber yarn contains ~1000 individual filaments. After their commercial synthesis, the fibers are coated with chemical agents generically called “fiber surface coating (FSC)” and frequently refered to in the jargon as “sizing” or “finish”. This coating reduces fiber damage when handled and improves the processability of the fibers [23]. The FSC formulation is complex and varies according to the final application and manufacturer; it may contain, among others, additives, lubricants, antistatic agents, emulsifiers and antioxidants [23].

Commercial MWCNTs were acquired from Cheaptubes Inc. (Vermont, USA), with a typical length of 1-6 µm, an inner average diameter of 5-15 nm and an outer average diameter of 30-50 nm [24]. Chemical oxidation of the MWCNTs was conducted with a mixture of H_2SO_4 (97.9 % v/v) and HNO_3 (65.4 % v/v) from J.T. Baker (Pennsylvania, USA). Chlorosulfonic acid at 97 % v/v from Merck & Co (New Jersey, USA) and dichloromethane 99.8 % v/v from Winkler LTDA (Santiago, Chile). To remove the FSC, ethanol and methanol 98 % v/v were acquired from Merck, acetone (98 % v/v) from Winkler LTDA and dichloromethane 99.8 % v/v also from Winkler LTDA. The deposition of MWCNTs onto the fiber surface was made with Chloroform at 99.9 % v/v from J.T. Baker.

2.2. Chemical oxidation of carbon nanotubes

All MWCNTs used in this work were chemically oxidiezed. A 3.0 M mixture of nitric and sulfuric acids was used for chemical oxidation of MWCNTs, using a previously reported method [25]. Briefly, the acid mixture and MWCNTs were first mechanically stirred in a hot plate for 15 min at ~ 60 °C. Then, the acid mixture and MWCNTs were ultrasonically dispersed using an ultrasonic bath of 70 W and 42 kHz for 2 h. The slurry was then filtered, thorougly washed with distilled water and dried at 100 °C for 24 h.

2.3. Aramid fiber treatments

The aramid fiber yarns used are classified into three groups, viz. as-received (without treatment) and treated by one of the two chemical modifications conducted herein. Prior to these chemical treatments, the FSC was removed by Soxhlet extraction and sequential inmersions in solvents as described in section 2.3.1. Then, the aramid fibers were subjected to a treatment with chlorosulfonic acid or to a (more aggressive) treatment using a mixture of nitric and sulfuric acids. Finally, previously oxidized MWCNTs were deposited on each of the three types of aramid fibers using a chloroform immersion method assisted by ultrasound. The following sections describe the removal of the FSC, the chemical treatments and the MWCNT deposition processes.

2.3.1. Removal of fiber surface coating

The FSC was removed by a Soxhlet extraction and secuential inmersions in chloroform, ethanol, acetone, and methanol, as recommended in [4]. The aramid fibers were dried in a convection oven at 70 °C after each sequential step. First, the aramid fibers were placed in a Soxhlet extractor recirculating chloroform for 6 h. The process was repeated in the Soxhlet extractor for 6 h using ethanol, and then with acetone and methanol. After removing the FSC, one of the two chemical treatments described below (sections 2.3.2 and 2.3.3) were applied to activate the fiber surface.

2.3.2. Fiber treatment by a mixture of nitric and sulfuric acids

The modification of the aramid fiber surface (with FSC previously removed, see section 2.3.1) was performed by immersing the yarn in a 3.0 M mixture of HNO_3 and H_2SO_4 for 1 h. Then, the aramid fibers were washed with 1.5 L of distilled water. This treatment is expected to affect the amorphous phase of the aramid fibers (< 24 %) through amide bond opening situated at the backbone of the fiber structure and the generation of amide and carboxyl groups in some fiber sections, see Figure 1 [26,27]. These functional groups can interact through hydrogen bonds with the carboxyl and hydroxyl groups of the previously oxidized MWCNTs [28].

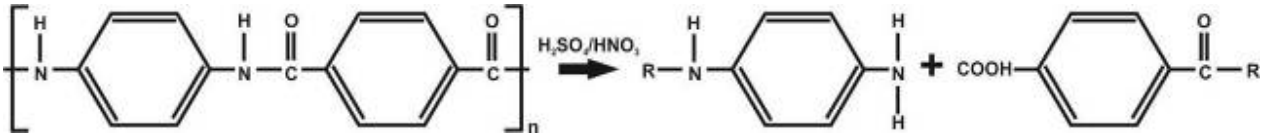

Figure 1. Proposed hydrolysis reaction for aramid fibers treated with the mixture of nitric and sulfuric acids.

2.3.3. Fiber treatment by chlorosulfonic acid

The aramid fibers whose FSC previously removed were treated with a solution of chlorosulfonic acid in dichlorometane at 0.2 % w/w, stirring the solution at room temperature for 2 min. Subsequently, the aramid fibers were inmmersed in distilled water stirring for 2 more min and finally dried for 1 h at 70 °C. This treatment is expected to produce sulfuryl chloride (SO_2Cl) groups in the active sites of the aromatic rings, see Figure 2. The subsequent inmersion in distilled water is expected to convert the sulfuryl chloride groups into sulfonic groups (SO_3H), as discussed in [4]. This treatment is also expected to modify the amorphous phase of the aramid fiber surface [26, 27]. The central amide group of the fiber can separate due to sulfonation yielding carboxylic functional groups (see Figure 2), which are expected to interact with the OH, COOH and CO functional groups of the oxidazed MWCNTs through hydrogen bonding [28].

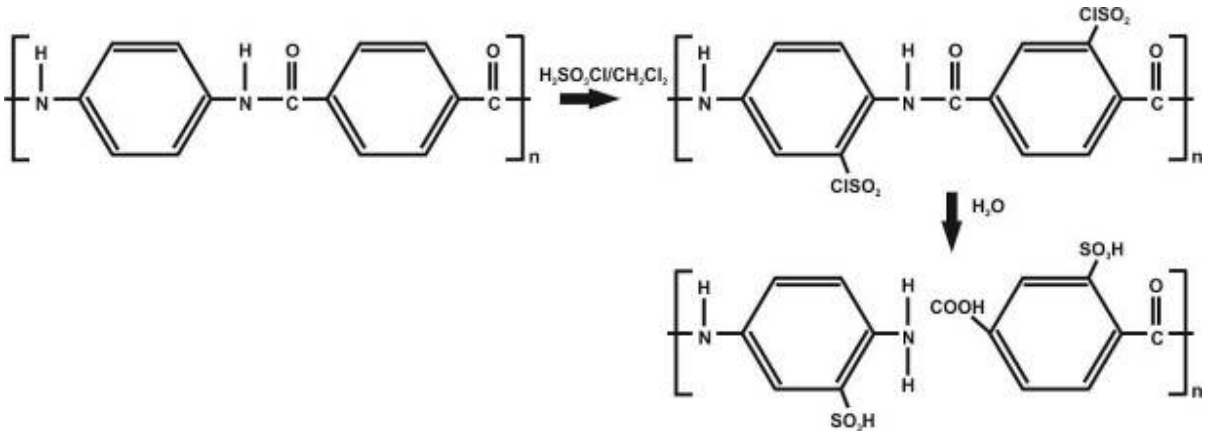

Figure 2. Proposed reaction for aramid fibers treated with chlorosulfonic acid.

2.4. Deposition of carbon nanotubes onto aramid fibers

Figure 3 shows the process used to deposit MWCNTs onto aramid fibers. 4 mg of previously oxidized MWCNTs were deposited onto ~ 550 mg of aramid fibers rolled on a cylindrical frame and inmmerded into 100 ml of chloroform. The MWCNT deposition onto aramid fibers was conducted by using an ultrasonic horn for 1 h at 165 W and 20 kHz. Finally, the aramid fibers were dried in a convection oven for 2 h at 100 °C.

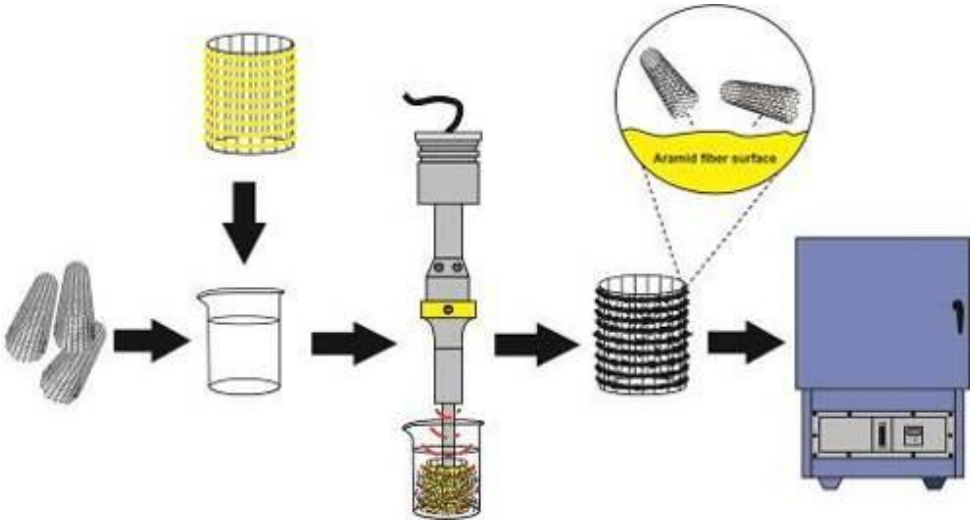

Figure 3. Schematic of the method used for the deposition of MWCNTs onto aramid fibers.

The nomenclature of the as-received, chemically modified and fibers with deposited MWCNTs used in the present study are described in Table 1.

Table 1. Nomenclature used for the aramid fibers without and with MWCNTs.

Label	Aramid fiber condition
TF	Pristine fibers (as-received).
TFAC	Fibers were immersed in a mixture of sulfuric and nitric acids for 3 h.
TFCL	Fibers were immersed in a solution of chlorosulfonic acid in dicloromethane for a few minutes.
TF-CNT	TF with deposited MWCNTs.
TFAC-CNT	TFAC with deposited MWCNTs.
TFCL-CNT	TFCL with deposited MWCNTs.

2.5. Fiber characterization

2.5.1. Infrared spectroscopy

Fourier transform infrared spectroscopy (FT-IR) was conducted using a Nicolet 8700, Thermo Fisher Scientific spectrometer. The FT-IR spectra of the samples were collected in the 650-4000 cm^{-1} interval with a resolution of 4 cm^{-1}. The samples were analyzed in the absorbance mode using KBr pellets. These analyzes were repeated 5 times finding reproducibility.

2.5.2 Raman spectroscopy

Raman spectroscopy of individual aramid fibers fixed in a cardboard frame was obtained by a micro Raman spectrometer equipped with an Andor DV401 CCD camera. A laser of 35 mV with a wavelength of 632.8 nm (1.96 eV) was used. Raman spectra were collected in the frequency range of 20-200 cm^{-1}. The analysis of individual Twaron fibers was conducted by mounting the fiber in a cardboard frame using adhesive tape. The total exposition time was 25 min.

The analysis of the MWCNT distribution on the fiber was performed using a WITec ALPHA 300R confocal Raman spectrophometer. Raman spectra of 30 × 45 pixeles were obtained with an exposition time of 2 s per pixel covering an area of 5 × 10 µm. For this maping, each pixel was generated by the intensity of the 2D Raman band of the MWCNTs at ~ 2700 cm^{-1} [31]. The images were processed using a WITec Project 2.08 software.

2.5.3 X-ray phoelectron spectroscopy

X-ray phoelectron spectroscopy (XPS) was carried out over aramid fiber tows using a sampling area of 400 µm by 400 µm. A Thermo Scientific K-Alpha™ X-ray photoelectron spectrometer with monochromatic Al Kα X-ray source operated with an energy of 1486.6 eV. The XPS survey scans were obtained by setting the analyzer to a 1 eV energy pass, while an energy pass of 0.1 eV was employed for high resolution windows. The high resolution C1s orbital curves were corrected by using a baseline obtained from a Shirley background [29, 30], and fitted using Voigt functions [29] to obtain additional information.

2.5.4 Scanning electron microscopy

Morphological analysis of the fiber surface and the analysis of the presence of MWCNTs on the fibers were performed by scanning electron microscopy. SEM analysis was performed by using a JEOL JSM-630-LV microscope at 20 kV.

2.6 Tensile testing

Tensile testing of individual Twaron fibers was conducted by mounting the fiber in a cardboard frame using adhesive tape and a commercial cyanoacrylate-based glue (Figure 4). Tests were conducted in an AG1-100 Shimadzu universal testing machine using a double sensitivity load cell of 100 N at cross-head speed of 1 mm/min. Since strain was measured with the machine cross-head displacement, a compliance correction was carried out for the elastic modulus (E) and

maximum strain (ε_{max}), using specimens with effective gauge lengths of 10, 20 and 40 mm, following the procedure described by Adams *et al.* [32].

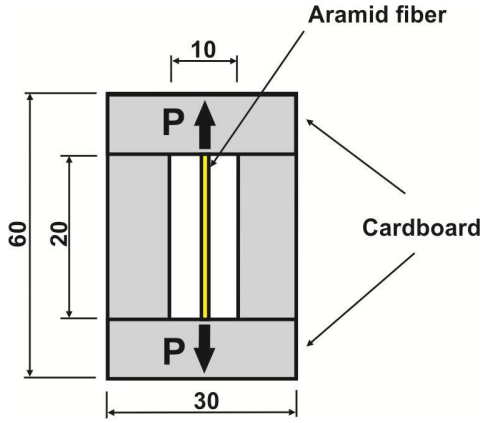

Figure 4. Setup used for tensile testing of individual fibers. Dimensions in mm. *P* shows the loading direction.

2.7 Electrical resistance measurements

Diecr current electrical resistance of MWCNT-modified aramid fiber yarns (comprising ~ 1000 individual fibers) was measured using a two point method. 15 mm long yarns were fixed in a cooper frame with an effective span of 10 mm, as shown in Figure 5. The yarn ends were bonded to the cooper electrodes using commercial conductive silver paint (Ted Pella Inc. type 16062, CA, USA) and the electrical resistance was measured using a Keithey 7517B electrometer.

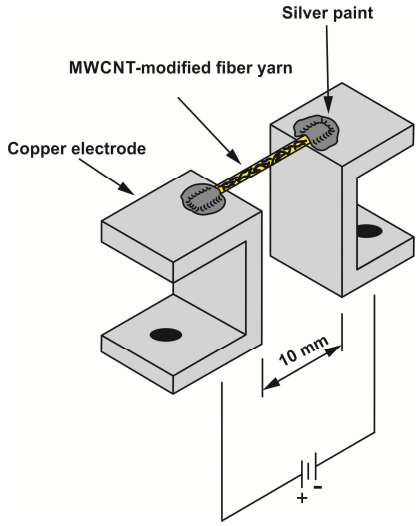

Figure 5. Setup used to measure the electrical resistance of MWCNT-modified aramid fiber yarns.

3. Results

3.1. Characterization of modified aramid fiber

3.1.1 Infrared spectroscopy

Figure 6 shows the FT-IR anaylsis of the as-received Twaron fibers (TF) and those with a chemical modification (TFCL and TFAC), as described in Table 1. Figure 6a shows the absorption bands of TF, TFAC and TFCL. The bands at 1123 cm^{-1} and 1305 cm^{-1} are attributed to stretching vibrations of C-N bonds [33]. The bands at 1514 cm^{-1} and 1636 cm^{-1} are attributed to stretching vibrations of N-H and C=O groups, respectively [33, 34]. The band at 1541 cm^{-1} is related to the combined motion of N-H bending and C-N [23]. The band at 3313 cm^{-1} is related to stretching vibrations of N-H of the amide groups [34]. Additionally, the band located at 820 cm^{-1} is asigned to stretching vibrations of the C-H bonds of the aromatic ring present in the backbone structure of the aramid fiber. This band does not present significant variations in intensity when the fiber is subjected to chemical treatments [23], and therefore was selected for normalization purposes. A detailed analysis in the interval 1200-1800 cm^{-1} is included in Figure 6b, where the intensities have been normalized with the intensity of the C-H band located at 820 cm^{-1}.

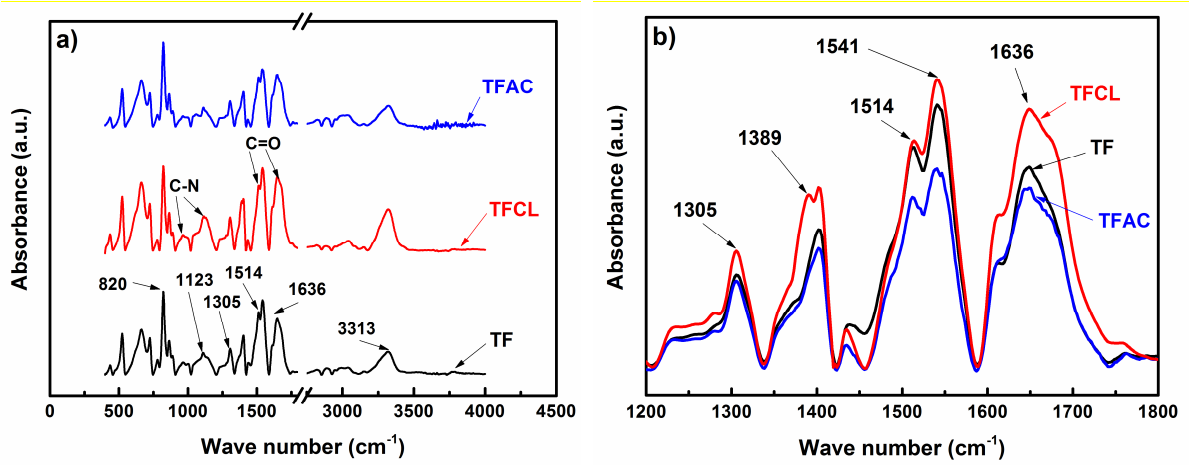

Figure 6. FT-IR analysis of aramid fibers without and with chemical treatment. a) Spectra of TF, TFCL and TFAC, b) 1200-1800 cm^{-1} region normalized with the 820 cm^{-1} band.

Figure 6b shows a slight increase in the intensity of the band at 1305 cm^{-1} (C-N) for TFCL with respect to TF, which can be attributed to the sulfonation of the aromatic rings [35]. Further indication of sulfonation is observed from a new band of small intensity at 1389 cm^{-1} for FTCL. The band at 1636 cm^{-1} also shows an increase in intensity for TFCL compared to TF, indicating fiber oxidation. The slight decrease in the C=O band at 1636 cm^{-1} for TFAC with respect to TF is

possibly caused by a competition between fiber oxidation and rupture of the bonds between the C=O and the N-H groups of the main aramid chain for such an aggresive fiber treatment [23]. Furter indication of rupture of the amide bonds for FTAC is observed by the intensity decrease of the bands at 1514 cm^{-1} and 1541 cm^{-1}, corresponding to N-H [35].

3.1.2 Raman spectroscopy

Figure 7 shows the results of Raman spectroscopy for TF, TFCL and TFAC. Figure 7a shows bands at 1185, 1280, 1332, 1520 and 1610 cm^{-1} related to stretching vibrations of the C-C bonds in the aromatic rings of the structure of the aramid fiber [36]. The band at 1571 cm^{-1} is attributed to stretching vibrations of the N-H bond. The vibrations at 1652 cm^{-1} are attributed to stretching modes of the C=O groups present in the main fiber structure [36]. The spectra of TFCL and TFAC are similar to that of TF, suggesting that the chemical treatments carried out do not significally modify the main structure of the aramid fiber. Since the Raman spectroscopy signal of the TF fiber is very intense (given its high crystallinity) and only a small amorphous phase at the fiber surface is expected to be modified by the chemical treatments, a surface change in the TF is difficult to determine by this technique.

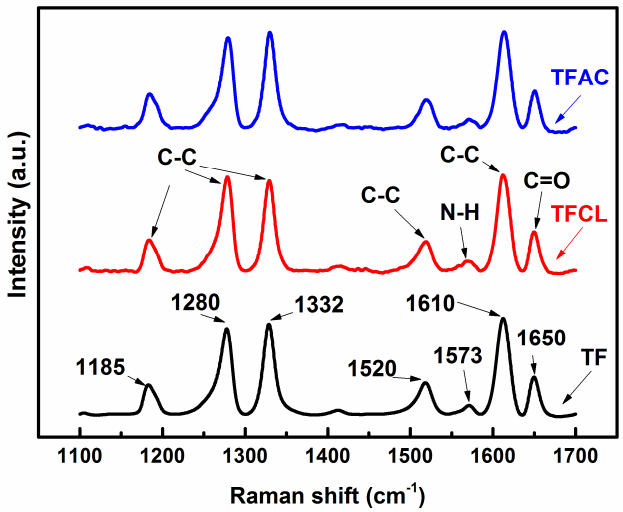

Figure 7. Raman spectra of as-received and chemically modified aramid fibers.

3.1.3 X-ray photoelectron spectroscopy

Figure 8 shows the XPS spectra of TF, TFCL and TFAC. These spectra show three high intensity bands corresponding to C1s, N1s and O1s orbitals at ~ 285, 400 and 532 eV, respectively [34, 37]. For TF, small bands assigned to sulfur at 105 and 156 eV are observed, which may stem from traces of the sulphuric acid employed in their synthesis process [5,37]. On the other hand, the bands at 105 and 156 eV in the TFAC fiber are generated by the acid treatment of the fiber

with sulfuric acid, as TFCL fibers do not exhibit such bands. For TFCL and TFAC a slight increase in intensity of the N1s orbital with respect to that of TF is observed. This increase is attributed to the removal of the FSC, which causes that a larger amount of nitrogen bonds become exposed on the fiber surface [6,38].

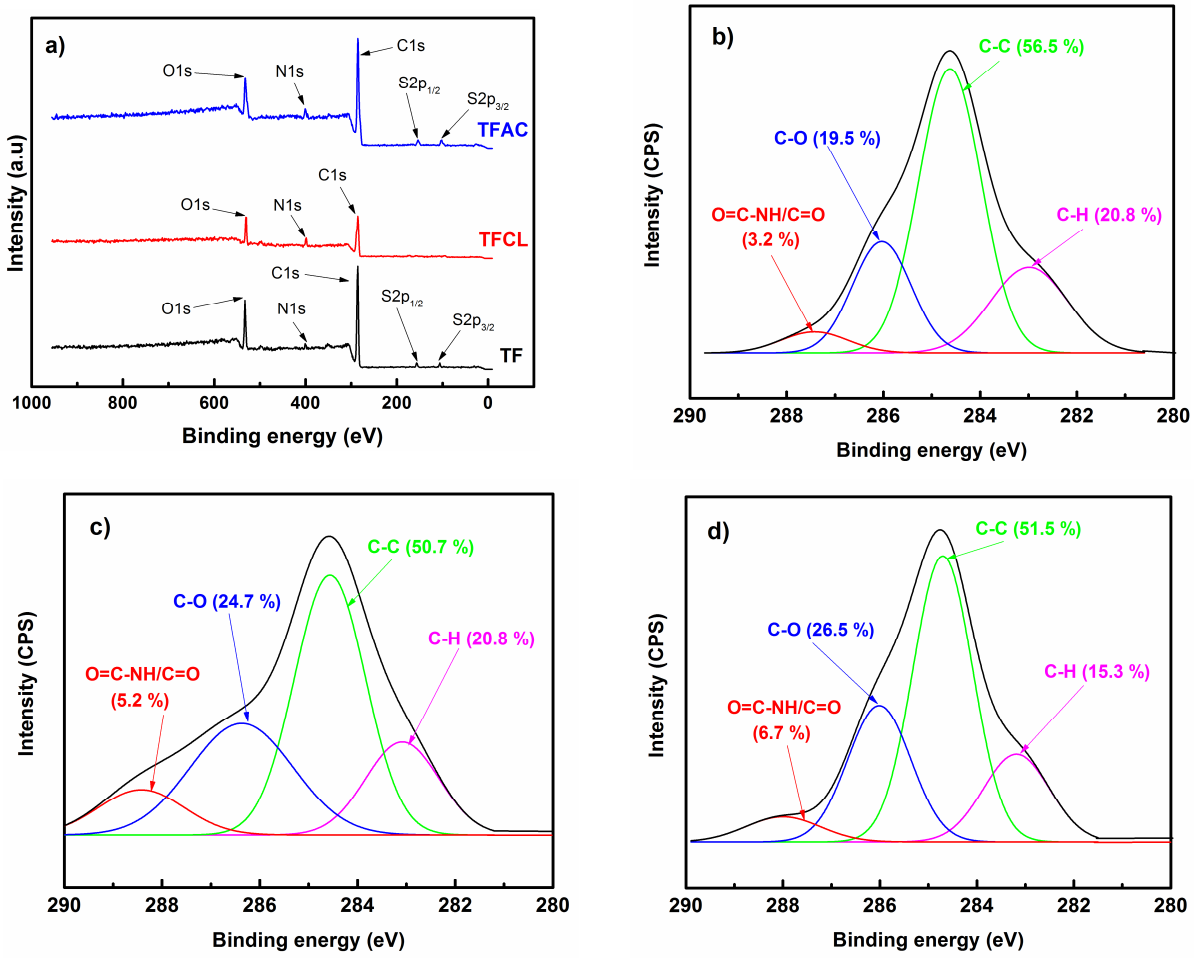

Figure 8. XPS analysis of as-received and chemically modified aramid fibers. a) Survey, b) C1s orbital of TF, c) C1s orbital of TFCL, d) C1s orbital of TFAC.

For a more detailed analysis, Figures 8b-d show deconvolutions of the C1s orbital (~ 285 eV) for all treatments, showing four bands; the first one from left to right located ~ 287.8 eV corresponds to the contribution of O=C-N-H and C=O bonds (3.2 %), coming from the amide and carbonyl functional groups present in the molecular structure of the aramid fiber [6]. Bands at ~ 286.0 and 284.6 eV are associated to C-O (19.5 %) and C-C (56.5 %) bonds, respectively, coming from the FSC and aromatic rings of the fiber [6,38]. Figures 8c and 8d show a deconvolution of the C1s orbital for TFCL and TFAC fibers, respectively. Because of the surface treatments, the proportions of the functional groups on the fiber surface significantly change with respect to the untreated fiber. For TFCL and TFAC fibers the contribution of O=C-N-H/C=O groups is larger, since the fiber is uncovered and depleted from the FSC, see e.g. [6,38]. For TF fibers, the

contribution of O=C-N-H bonds is 3.2 %, while for TFCL and TFAC is 5.2 % and 6.7 %, respectively; this suggests that the FSC has been removed and that the treatement based on the acid mixture generates more oxygen-containing functional groups, being more aggressive. Evidence of fiber chemical oxidation is observed from the increase of oxygen-containing functional groups such as C-O. These functional groups contribute to the C1s orbital in 19.5 % for TF, and their contribution greatly increase to 24.7 % for TFCL and 26.5 % for TFAC. This indicates that the TFAC fiber has higher degree of oxidation than TF and TFCL.

3.1.4. Scanning electron microscopy

Figure 9 shows SEM micrographs of aramid fiber yarns taken at 100x, 1000x and 5000x magnifications (from left to right). The as-received aramid fiber (Figure 9a) shows a relative smoth surface with shallow longitudinal markings produced by their synthesis process. TFCL fibers (Figure 9b) show similar characterictics to TF but they show new surface markings and the presence of some irregular material (particles) on the fiber surface. This material may correspond to traces of the FSC removed by Soxhlet extraction and by the subsequent chemical treatment carried out. The acid treatment (TFAC) was more aggresive with the fiber surface, which is evident in Figure 9c by the peeling off of some surface layers.

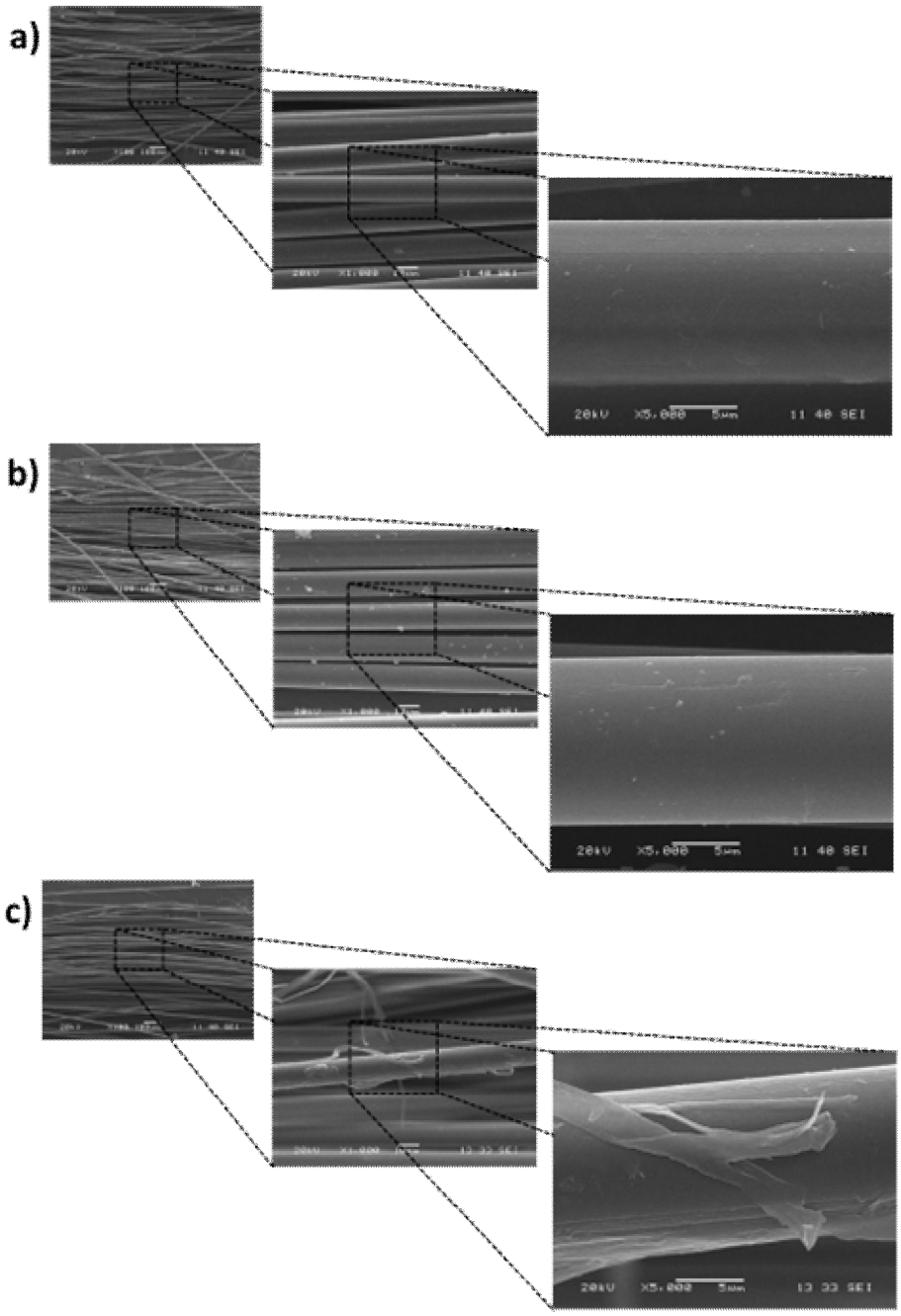

Figure 9. SEM micrographs of the as-received and treated aramid fibers.

a) TF, b) TFCL, c) TFAC.

3.1.5. Mechanical properties

Tensile stress (σ) vs. strain (ε) curves of the as-received (TF) and chemically modified (TFAC and TFCL) fibers with gauge lengths of 20 mm are presented in Figure 10. Table 2 summarizes the mechanical properties (average and standard deviation) obtained from such curves, listing the elastic modulus (E), strength (σ_{max}) and the maximun strain (ε_{max}).

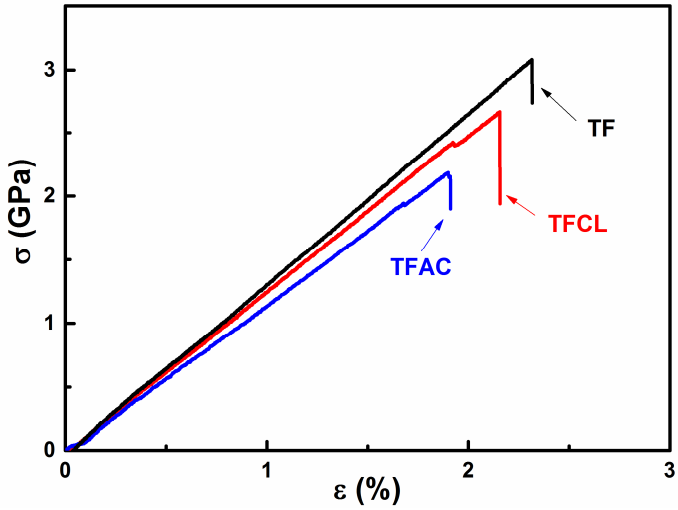

Figure 10. Representative stress-strain curves of individual aramid fibers TF, TFCL and TFAC.

E, σ_{max} and ε_{max} measured for the as-received fibers are similar to that reported in the literature [5]. According to the results of Figure 10 and Table 2, TF and TFCL show statistically similar mechanical properties, although the ones treated with chlorosulfonic acid show a trend to reduce their mechanical properties. On the other hand, fibers treated with the acid mixture (TFAC) show a more considerable reduction in E, σ_{max} and ε_{max} with respect to TF. These results are consistent with the ones obtained from FT-IR, XPS and SEM, all suggesting that the treatment with nitric and sulphuric acids is more oxidative and also damages more the aramid fibers.

Table 2. Tensile properties of as-received and chemically modified aramid fibers.

Fiber	***E*** **(GPa)**	σ_{max} **(GPa)**	ε_{max} **(%)**
TF	167 ± 25.3	2.70 ± 0.33	2.47 ± 0.50
TFCL	134 ± 10.8	2.56 ± 0.31	2.01 ± 0.22
TFAC	124 ± 5.0	1.97 ± 0.40	1.76 ± 0.29

3.2. Characterization of MWCNT-modified aramid fibers

3.2.1 Raman spectroscopy

Figure 11 shows the Raman spectra of MWCNT-modified aramid fibers. Figure 11a shows the spectrum of the oxidized MWCNTs (bottom, labeled as "CNT") and of the TF, TFCL and TFAC fibers containing MWCNTs on their surface. The typical D and G bands of the MWCNTs are observed at 1335 and 1587 cm^{-1}, respectively [31]. The spectra of the MWCNT-modified fibers TF-CNT, TFCL-CNT and TFAC-CNT show two bands at 1281 and 1610 cm^{-1} corresponding to the C-C vibration of the aromatic rings of the molecular structure of the aramid fiber (see Figure 7). These bands belonging to the fibers overlap the D and G bands of the MWCNTs, and consequently, their intensity and width increase when MWCNTs are deposited on the fiber surface, as shown in Figures 11 b-d for the band centerd at 1610 cm^{-1}.

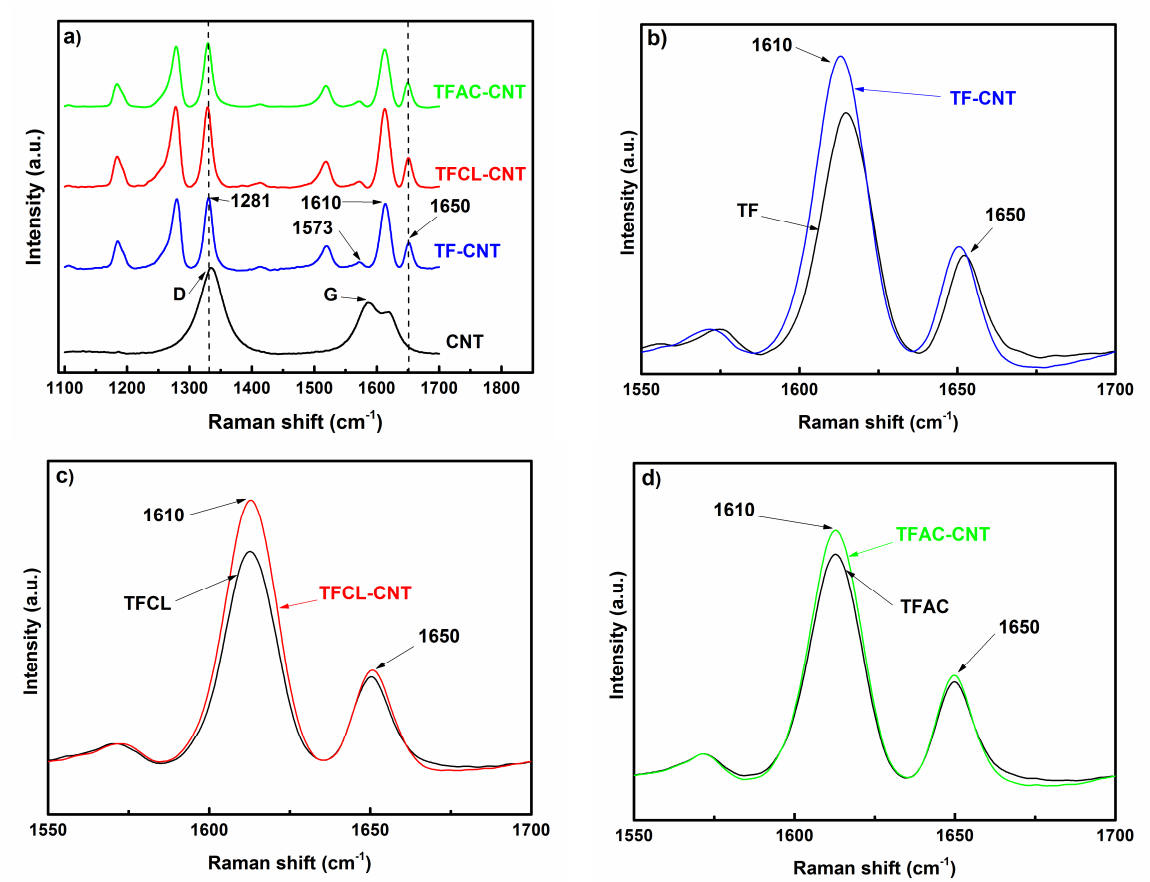

Figure 11. Raman spectra of the aramid fibers. a) MWCNTs (CNT), TF-CNT, TFCL-CNT and TFAC-CNT, b) TF and TFCNT, c) TFCL and TFCL-CNT, d) TFAC and TFAC-CNT.

For a more detaild analysis of the band at 1610 cm^{-1}, the 1550-1700 cm^{-1} spectral range was further investigated (see Figures 11 b-d), normalizing the band intensities with the intensity of the band at 1571 cm^{-1}, which is attributed to N-H vibrations. As observed form these figures, the presence of MWCNTs on the TF-CNT, TFCL-CNT and TFAC-CNT fibers increases the intensity and width of the band at 1610 cm^{-1}, with respect to the fibers without MWCNTs. To quantify this observation the area under the band at 1610 cm^{-1} (A_{1610}) was divided by the corresponding area under the band at 1571 cm^{-1} (A_{1571}), taken as reference. Table 3 shows the results of this metric, reporting average and standard deviations corresponding to 5 replicates. The last column represents the increase (with respect to averages) of the A_{1610}/A_{1571} ratio for the fiber with MWCNTs (TF-CNT, for instance) relative to its corresponding fiber without MWCNTs (TF, for instance). This parameter may be interpreted as an indicator of the amount of MWCNTs on the fiber surface. As shown in Table 3, the as-received fiber and the fiber treated with chlorosulfonic acid (TFCL) present higher amounts of MWCNTs deposited on their surface (ratios of 20.3 and 18.7, respectively). In the case of TF, the functional groups present in the oxidized MWCNTs (OH, C-O and COOH) interact with the oxygen-containing functional groups present in the FSC of the as-received fiber, as reported for glass and carbon fibers [19,38]. Twaron fibers have a standard surface coating which comprises a non-ionic emulsifier containing large molecules with ramifications of ethylene and propylene oxide functional groups, as well as hydroxyl and carboxyl groups [39,40]. Upon ultrasonic MWCNT deposition, the temperature is raised to ~70 °C and the hydroxyl and carboxyl groups of the oxidized MWCNTs can covalently react with the ethylene and propylene oxides through anionic ring-opening reactions [41]. These ring-opening reactions yield new hydroxyl groups, which could also react with the hydroxyl and carboxyl groups on the MWCNT surface through hydrogen bonding [19].
On the other hand, according to the increase in the area ratio of 18.7 %, the chlorosulfonic treatment also promotes good affinity between the treated fibers and the oxidized MWCNTs, being mild with the fiber. In contrast, the acid treatment TFAC is aggressive with the fiber and concomitant with the remotion of the FSC renders the lowest amount of MWCNTs per area (9.6 % increase).

Table 3. Area under the curve of the band at 1610 cm^{-1} normalized by the area of the band at 1571 cm^{-1}.

Fiber	A_{1610}/A_{1571}	Area increment with respect to the corresponding fiber without MWCNTs (%)
TF	211 ± 4.6	-
TF-CNT	254 ± 9.8	20.3
TFCL	238 ± 10.3	-
TFCL-CNT	284 ± 11.5	18.7
TFAC	190 ± 2.6	-
TFAC-CNT	208 ± 8.8	9.6

3.2.2 X-ray photoelectron spectroscopy

Figure 12 shows the XPS results of TF-CNT, TFCL-CNT and TFAC-CNT fibers. Figure 12a shows surveys of the fibers with deposited MWCNTs. These spectra show high intensity bands corresponding to C1s, N1s and O1s orbitals; additionally, the spectra show a few low intensity bands corresponding to traces of metals, likely from the MWCNT synthesis [24,42].

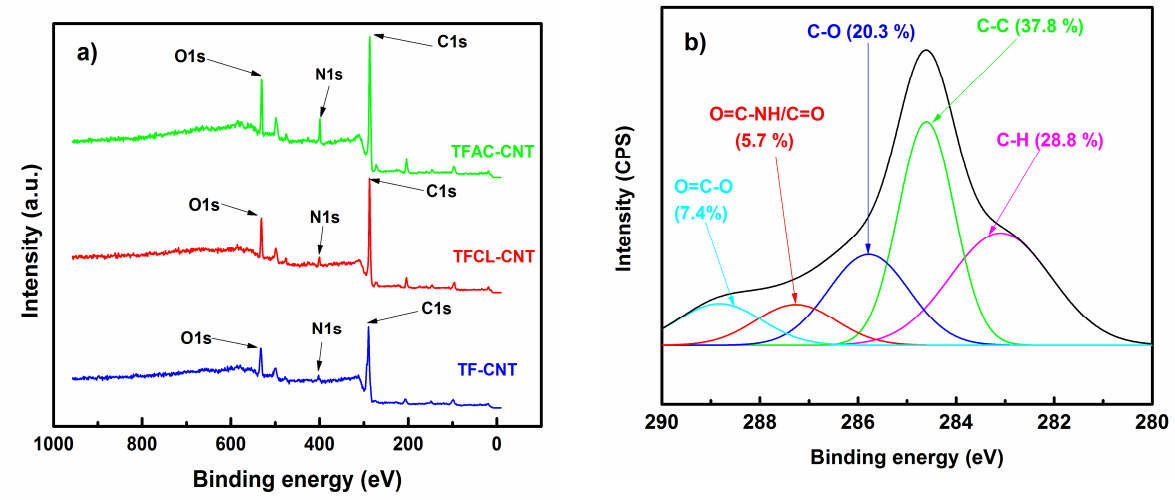

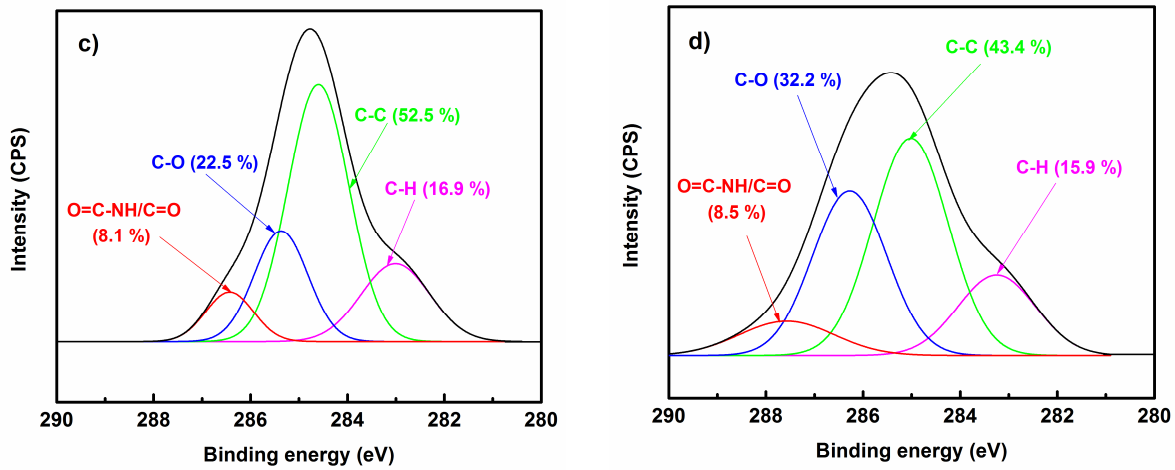

Figure 12. XPS spectra of MWCNT-modified aramid fibers. a) Surveys, b) C1s orbital of TF-CNT, c) C1s orbital of TFCL-CNT, d) C1s orbital of TFAC-CNT.

A more detailed analysis is obtained by examining the deconvolution of the C1s band shown in Figures 12b-d. In Figure 12b five bands are observed corresponding to O=C-O (289 eV), O=C-NH/C=O (287.8 eV), C-O (286 eV), C-C (284.6 eV) [6] and C-H (283 eV) [43]. The first one from left to right, located ~ 289 eV corresponds to the contribution of C=O and C-O bonds (7.4 %), probably coming from the interaction between the functional groups of the oxidized MWCNTs and the FSC. This band was not observed in Figures 12 c-d (TFCL-CNT and TFAC-CNT), where the FSC was removed. The emergence of a new band at ~289 eV in as-received fibers after MWCNT deposition suggests an interaction between the FSC and the MWCNTs, as has been previously reported [19,44]. The increase of the intensity of the band at ~ 287.8 eV (O=C-NH/C=O) in Figures 12b-d in comparison to the fibers without MWCNTs (Figures 8b-8d) suggests the presence of oxidized MWCNTs. The band at ~ 286 eV corresponds to C-O bonds. Its contribution is higher for TFCL-CNT (22.5 %, Figure 12c) than for TF-CNT (20.3 %, Figure 12a) and even higher for TFAC-CNT (32.2 %, Figure 12d), suggesting an increased contribution of the C-O bonds coming from the oxidation of the aramid fibers and the oxidized MWCNTs.

3.2.3. Scanning electron microscopy

Figure 13 shows SEM micrographs of the aramid fiber yarns with MWCNTs deposited on their surface at magnifications of 100×, 1000× and 5000× (left to right). Figure 13a shows as-received fibers with deposited MWCNTs (TF-CNT), showing a relatively homogeneous distribution of MWCNTs over the TF surface; a few agglomerations are observed in some regions. Figure 13b shows SEM micrographs of TFCL-CNT fibers, where again a rather homogeneous distribution

of MWCNTs on the fiber surface with less agglomerates is observed. However, Figure 13c shows that for TFAC-CNT fibers the MWCNT distribution is significanlty less homogeneous than for TF-CNT and TFCL-CNT fibers. This is probably caused by the removal of the FSC and the presence of high density of functional groups in localized areas of the fiber surface. These results are in agreement with the results of Raman spectroscopy and XPS.

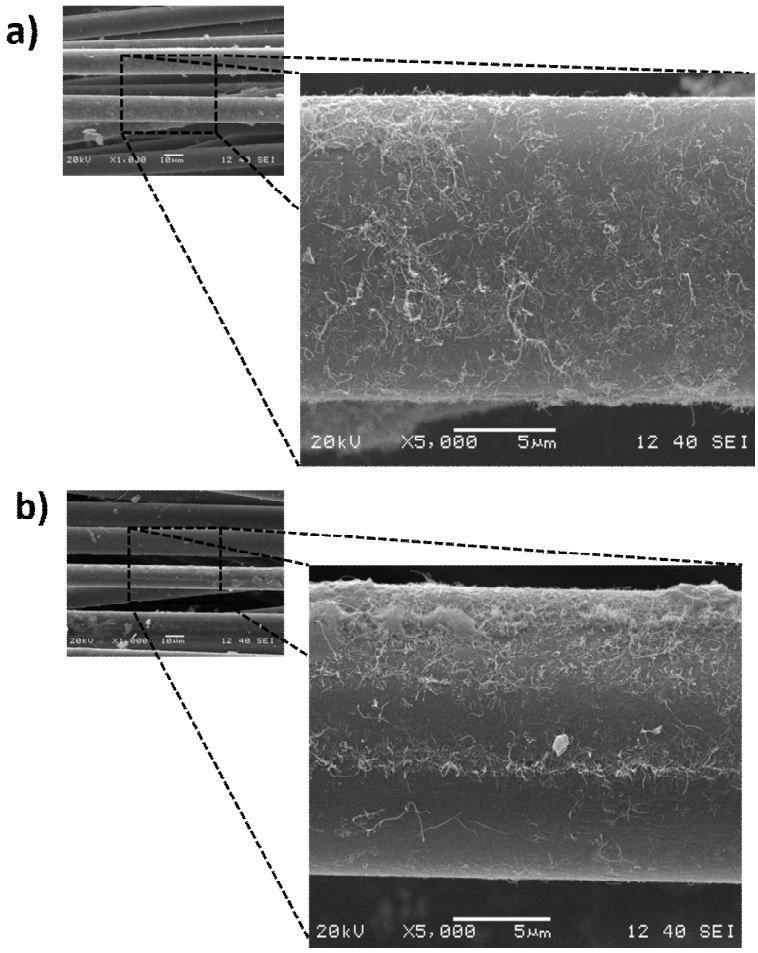

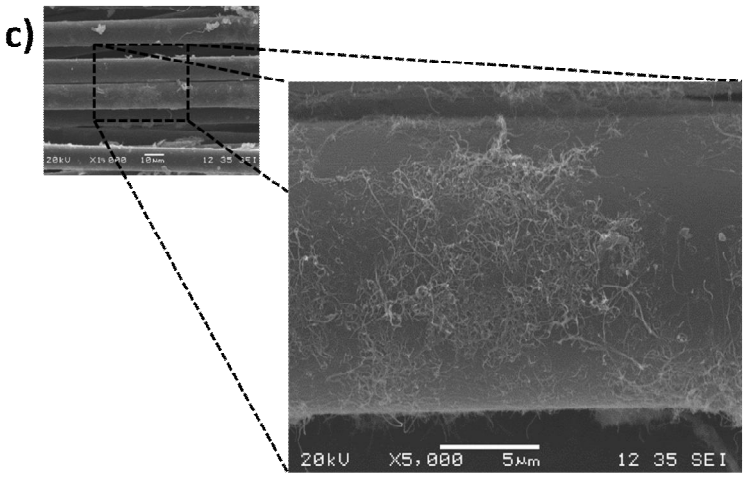

Figure 13. SEM micrographs of MWCNT-modified aramid fibers. a) TF-CNT, b) TFCL-CNT, c) TFAC-CNT.

3.2.4. Raman spectroscopy mapping

Figure 14 shows Raman mapping of the aramid fiber surface containing the deposited MWCNTs. Bright regions represent areas of high intensity of the MWCNT 2D band, while dark regions are fiber areas with low intensity of such a band, i.e. low density of MWCNTs. Mapping the TF-CNT fiber surface (Figure 14a) consistently shows many MWCNT-rich zones. The distribution of MWCNTs on the fiber surface looks relatively more homogenous for TFCL-CNT (Figure 14b), given the mild chlorosulfonic acid treatment carried out. However, the map of the TFAC-CNT fibers (Figure 14c) evidence larger MWCNT agglomerations, likely due to the removal of the FSC and the aggressiveness of the fiber treatment, leading to localized active regions. These results are again in agreement with the SEM and physicochemical characterizations presented earlier.

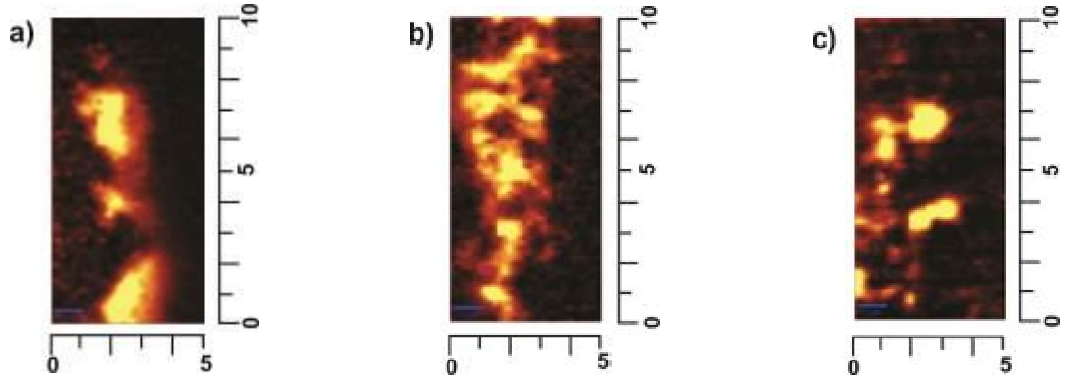

Figure 14. 2D Raman band intensity maps of the MWCNTs on the aramid fiber surface. a) TF-CNT, b) TFCL-CNT, c) TFAC-CNT. Dimensions in µm.

3.2.5. Electrical resistance of MWCNT-modified fibers

Twaron fibers are electrically insulating materials with conductivity of the order of 1×10^{-15} S/cm [45]. Upon MWCNT deposition, the surface of the twaron fibers became electrically conductive. Figure 15 shows the electrical resistances of 10 mm long fiber yarns for TF-CNT, TFCL-CNT and TFAC-CNT fibers. After the deposition of MWCNTs, the majority of the electrical resistance values of the three samples fall in the range of 200 kΩ to 50 MΩ, and a few TF-CNT fibers reach ~100 kΩ. MWCNTs deposited onto the surface of aramid fibers promote the formation of electrically conductive pathways among adyacent fibers and along the yarn, and the chemical treatment does not seem to yield an important global effect in the surface conductivity of the fiber. The data scattering might seem high, but this experimental scattering is reasonable considering the challenges involved in the deposition of MWCNTs onto engineering fibers, due to the difficulty of homogeneously depositing MWCNTs at the nano- and micro-scales (see e.g. [20]). This electrical property confers multifunctional capabilities to the aramid fibers, such as the ability to be used as electrical filaments [46,47], as strain sensors [48] or for "structural health" monitoring in multiscale hierarchical composites [49,50].

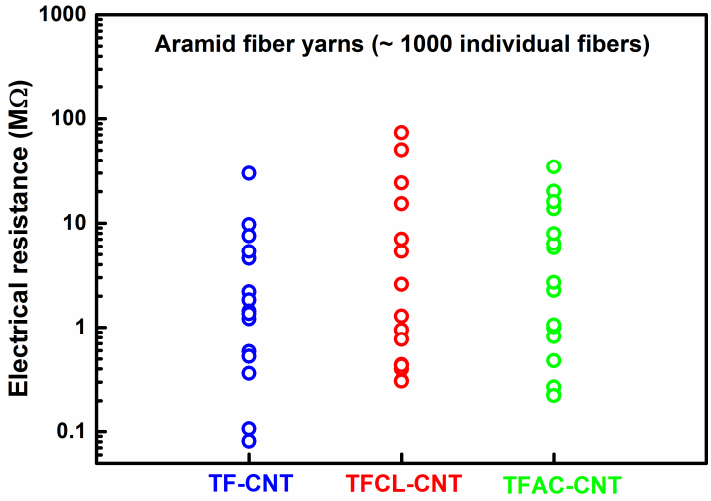

Figure 15. Electrical resistance of TF-CNT, TFCL-CNT and TFAC-CNT fibers.

4. Conclusions

Oxidized multiwall carbon nanotubes were deposited on as-received (commercial) Twaron fibers and on chemically modified Twaron fibers (with "sizing" removed) using chorosulfonic acid at 0.2 % w/w or using a mixture of nitric and sulfuric acids at 3.0 M. FT-IR and Raman analyses showed certain evidence of the success of the chemical treatments, but the surface changes

detected by these techniques were only moderate due to the high crystallinity of the aramid fiber. XPS, however, showed conspicuous evidence of fiber surface changes produced by both chemical treatments. O=C-NH/C=O and C-O functional groups were observed in higher proportion for fibers modified with the nitric and sulfuric acids mixture, in comparison to those generated for fibers treated with the chorosulfonic acid or as-received. This suggests that the fiber modification based on the nitric and sulfuric acids mixture generates more functional groups, but is also more agressive. Both chemical treatments modified the mechanical properties of the fibers. The reduction of strength, ultimate strain, and elastic modulus of the fibers treated with chorosulfonic acid was small. However, those treated with the mixture of nitric and sulfuric acids experienced more important reductions in their mechanical properties.

Regarding MWCNT deposition on the surface of aramid fibers, Raman spectroscopy and XPS presented conspicuous evidence of the MWCNT deposition on the aramid fiber. The results suggest that the presence of the fiber surface coating or a mild chlorosulfonic treatment promote increased interactions between the fiber and oxidized MWNCTs. Confirmation of these results was obtained by SEM images and Raman intensity maps, pointing towards a more homogeneous distribution of MWCNTs on the fiber surface for fibers without treatment and for those treated with chlorosulfonic acid.

The results of electrical resistance measurements of 10 mm long fiber yarns span over similar values (0.2-50 MΩ) for as-received or chemically modified fibers. The similarility of these values regardless of the fiber treatment suggests that the establishment of electrically percolative networks occurs predominantly by side-contact between adyacent fibers, and is not greatly affected by the fiber treatment. The electrical resistance of the fiber yarns (~200 kΩ/cm) and their excelent mechanical properties render multifunctional properties that may be exploited in applications related to energy storage and transportation, as well as structural elements in multiscale hierarchical composites which are able to self-sense their damage.

Acknowledgements

This research is part of a Mexico-Chile collaborative project supported by CONACYT-CIAM (Mexico, No. 188089) and CONICYT (Chile, No. 120003) directed by Dr. Avilés and Dr. Yazdani-Pedram. Input of Dr. Juan V. Cauich regarding the chemical treatments is strongly appreciated. Support in the form of a grant to our graduate school program from the “Fondo

Mixto CONACYT-Gobierno del Estado de Yucatán", project No. 247046, is also acknowledged.

Technical assistance of Cesar Martin and Alejandro May (CICY) is also strongly appreciated.

References

[1] H.G. Chae, S. Kumar, Rigid-rod polymeric fibers, Journal of Applied Polymer Science, 100 (2006) 791-802.

[2] D. Tanner, J.A. Fitzgerald, B.R. Phillips, The Kevlar Story—an Advanced Materials Case Study, Angewandte Chemie International Edition in English, 28 (1989) 649-654.

[3] W. Chen, X.M. Qian, X.Q. He, Z.Y. Liu, J.P. Liu, Surface modification of Kevlar by grafting carbon nanotubes, Journal of Applied Polymer Science, 123 (2012) 1983-1990.

[4] T. Lin, S. Wu, J. Lai, S. Shyu, The effect of chemical treatment on reinforcement/matrix interaction in Kevlar-fiber/bismaleimide composites, Composites Science and Technology, 60 (2000) 1873-1878.

[5] M. Jassal, S. Ghosh, Aramid fibres-An overview, Indian Journal of Fibre and Textile Research, 27 (2002) 290-306.

[6] C. Jia, P. Chen, B. Li, Q. Wang, C. Lu, Q. Yu, Effects of Twaron fiber surface treatment by air dielectric barrier discharge plasma on the interfacial adhesion in fiber reinforced composites, Surface and Coatings Technology, 204 (2010) 3668-3675.

[7] C.X. Wang, M. Du, J.C. Lv, Q.Q. Zhou, Y. Ren, G.L. Liu, D.W. Gao, L.M. Jin, Surface modification of aramid fiber by plasma induced vapor phase graft polymerization of acrylic acid. I. Influence of plasma conditions, Applied Surface Science, 349 (2015) 333-342.

[8] J. Chen, Y. Zhu, Q. Ni, Y. Fu, X. Fu, Surface modification and characterization of aramid fibers with hybrid coating, Applied Surface Science, 321 (2014) 103-108.

[9] S. Hussain, C. Yorucu, I. Ahmed, R. Hussain, B. Chen, M. Bilal Khan, N.A. Siddique, I.U. Rehman, Surface modification of aramid fibres by graphene oxide nano-sheets for multiscale polymer composites, in: Surface and Coatings Technology, (2014) 458-466.

[10] M. Xi, Y.-L. Li, S.-y. Shang, D.-H. Li, Y.-X. Yin, X.-Y. Dai, Surface modification of aramid fiber by air DBD plasma at atmospheric pressure with continuous on-line processing, Surface and Coatings Technology, 202 (2008) 6029-6033.

[11] T. Ai, R. Wang, W. Zhou, Effect of grafting alkoxysilane on the surface properties of Kevlar fiber, Polymer composites, 28 (2007) 412-416.

[12] J. Gao, Y. Dai, X. Wang, J. Huang, J. Yao, J. Yang, X. Liu, Effects of different fluorination routes on aramid fiber surface structures and interlaminar shear strength of its composites, Applied Surface Science, 270 (2013) 627-633.

[13] S. Wu, G. Sheu, S. Shyu, Kevlar fiber–epoxy adhesion and its effect on composite mechanical and fracture properties by plasma and chemical treatment, Journal of applied polymer science, 62 (1996) 1347-1360.

[14] J. Maity, C. Jacob, C. Das, A. Kharitonov, R. Singh, S. Alam, Fluorinated aramid fiber reinforced polypropylene composites and their characterization, Polymer composites, 28 (2007) 462-469.

[15] J. Guo, C. Lu, Continuous preparation of multiscale reinforcement by electrophoretic deposition of carbon nanotubes onto carbon fiber tows, Carbon, 50 (2012) 3101-3103.

[16] S. Zhang, W. Liu, L. Hao, W. Jiao, F. Yang, R. Wang, Preparation of carbon nanotube/carbon fiber hybrid fiber by combining electrophoretic deposition and sizing process for enhancing interfacial strength in carbon fiber composites, Composites Science and Technology, 88 (2013) 120-125.

[17] L. Liu, P.-C. Ma, M. Xu, S.U. Khan, J.-K. Kim, Strain-sensitive Raman spectroscopy and electrical resistance of carbon nanotube-coated glass fibre sensors, Composites Science and Technology, 72 (2012) 1548-1555.

[18] J. Zhang, R. Zhuang, J. Liu, E. Mäder, G. Heinrich, S. Gao, Functional interphases with multi-walled carbon nanotubes in glass fibre/epoxy composites, Carbon, 48 (2010) 2273-2281.

[19] J. Ku-Herrera, F. Avilés, A. Nistal, J. Cauich-Rodríguez, F. Rubio, J. Rubio, P. Bartolo-Pérez, Interactions between the glass fiber coating and oxidized carbon nanotubes, Applied Surface Science, 330 (2015) 383-392.

[20] J. Rausch, E. Mäder, Health monitoring in continuous glass fibre reinforced thermoplastics: Manufacturing and application of interphase sensors based on carbon nanotubes, Composites Science and Technology, 70 (2010) 1589-1596.

[21] N.A. Siddiqui, M.-L. Sham, B.Z. Tang, A. Munir, J.-K. Kim, Tensile strength of glass fibres with carbon nanotube–epoxy nanocomposite coating, Composites Part A: Applied Science and Manufacturing, 40 (2009) 1606-1614.

[22] I. O'Connor, H. Hayden, J.N. Coleman, Y.K. Gun'ko, High-Strength, High-Toughness Composite Fibers by Swelling Kevlar in Nanotube Suspensions, Small, 5 (2009) 466-469.

[23] G. Derombise, L. Vouyovitch Van Schoors, M.F. Messou, P. Davies, Influence of finish treatment on the durability of aramid fibers aged under an alkaline environment, Journal of Applied Polymer Science, 117 (2010) 888-898.

[24] F. Avilés, A. May-Pat, G. Canché-Escamilla, O. Rodríguez-Uicab, J.J. Ku-Herrera, S. Duarte-Aranda, J. Uribe-Calderon, P.I. Gonzalez-Chi, L. Arronche, V. La Saponara, Influence of carbon nanotube on the piezoresistive behavior of multiwall carbon nanotube/polymer composites, Journal of Intelligent Material Systems and Structures, (2014) 1-12.

[25] F. Avilés, J.V. Cauich-Rodríguez, L. Moo-Tah, A. May-Pat, V.-C. R, Evaluation of mild acid oxidation treatments for MWCNT functionalization, Carbon, 47 (2009) 2970-2975.

[26] E. Chatzi, J. Koenig, Morphology and structure of Kevlar fibers: a review, Polymer-Plastics Technology and Engineering, 26 (1987) 229-270.

[27] R. Uppal, G.N. Ramaswamy, T. Loughin, A novel method to assess degree of crystallinity of aramid filament yarns, Journal of Industrial Textiles, (2012) 3-19.

[28] I. O'Connor, H. Hayden, S. O'Connor, J.N. Coleman, Y.K. Gun'ko, Kevlar coated carbon nanotubes for reinforcement of polyvinylchloride, Journal of Materials Chemistry, 18 (2008) 5585-5588.

[29] S. Hofmann, Practice of Surface and Interface Analysis with AES and XPS, in: Auger- and X-Ray Photoelectron Spectroscopy in Materials Science, Springer Berlin Heidelberg, 2013, pp. 409-449.

[30] S. Tougaard, Quantification of surface and near-surface composition by AES and XPS, Handbook of Surface and Interface Analysis–Methods for Problem-Solving, CRC Press Taylor & Francis Group, Boca Raton, (2009) 223-244.

[31] M.S. Dresselhaus, G. Dresselhaus, R. Saito, A. Jorio, Raman spectroscopy of carbon nanotubes, Physics reports, 409 (2005) 47-99.

[32] D.F. Adams, L.A. Carlsson, R.B. Pipes, Experimental Characterization of Advanced Composite Materials, Boca Ratón, Florida, 2003.

[33] J. Maity, C. Jacob, C. Das, S. Alam, R. Singh, Direct fluorination of Twaron fiber and the mechanical, thermal and crystallization behaviour of short Twaron fiber reinforced polypropylene composites, Composites Part A: Applied Science and Manufacturing, 39 (2008) 825-833.

[34] J. Zhao, Effect of surface treatment on the structure and properties of para-aramid fibers by phosphoric acid, Fibers and Polymers, 14 (2013) 59-64.

[35] T. Lin, B. Kuo, S. Shyu, S.-H. Hsiao, Improvement of the adhesion of Kevlar fiber to bismaleimide resin by surface chemical modification, Journal of adhesion science and technology, 13 (1999) 545-560.

[36] L. Penn, F. Milanovich, Raman spectroscopy of Kevlar 49 fibre, Polymer, 20 (1979) 31-36.

[37] L.E. Hamilton, P. Sherwood, B.M. Reagan, X-ray photoelectron spectroscopy studies of photochemical changes in high-performance fibers, Applied spectroscopy, 47 (1993) 139-149.

[38] L. Liu, Q. Jiang, T. Zhu, X. Guo, Y. Sun, Y. Guan, Y. Qiu, Influence of moisture regain of aramid fibers on effects of atmospheric pressure plasma treatment on improving adhesion with epoxy, Journal of applied polymer science, 102 (2006) 242-247.

[39] P. De Lange, P. Akker, A. Maas, A. Knoester, H. Brongersma, Adhesion activation of Twaron® aramid fibres studied with low-energy ion scattering and x-ray photoelectron spectroscopy, Surface and interface analysis, 31 (2001) 1079-1084.

[40] P.J. De Lange, E. Mäder, K. Mai, R.J. Young, I. Ahmad, Characterization and micromechanical testing of the interphase of aramid-reinforced epoxy composites, Composites Part A: Applied Science and Manufacturing, 32 (2001) 331-342.

[41] M.S. Thompson, T.P. Vadala, M.L. Vadala, Y. Lin, J.S. Riffle, Synthesis and applications of heterobifunctional poly(ethylene oxide) oligomers, Polymer, 49 (2008) 345-373.

[42] V.N. Popov, Carbon nanotubes: properties and aplications, Materials Science and Technology, 43 (2004) 61-102.

[43] S.-H. Zhang, G.-Q. He, G.-Z. Liang, H. Cui, W. Zhang, B. Wang, Comparison of F-12 aramid fiber with domestic armid fiber III on surface feature, Applied surface science, 256 (2010) 2104-2109.

[44] M. Li, Y. Gu, Y. Liu, Y. Li, Z. Zhang, Interfacial improvement of carbon fiber/epoxy composites using a simple process for depositing commercially functionalized carbon nanotubes on the fibers, Carbon, 52 (2013) 109-121.

[45] K.K. Chang, Aramid fibers, Materials Park, OH: ASM International, (2001) 41-45.

[46] N. Behabtu, C.C. Young, D.E. Tsentalovich, O. Kleinerman, X. Wang, A.W. Ma, E.A. Bengio, R.F. ter Waarbeek, J.J. de Jong, R.E. Hoogerwerf, Strong, light, multifunctional fibers of carbon nanotubes with ultrahigh conductivity, Science, 339 (2013) 182-186.

[47] C. Xiang, W. Lu, Y. Zhu, Z. Sun, Z. Yan, C.-C. Hwang, J.M. Tour, Carbon Nanotube and Graphene Nanoribbon-Coated Conductive Kevlar Fibers, ACS Applied Materials & Interfaces, 4 (2011) 131-136.

[48] G.J. Ehlert, H.A. Sodano, Fiber strain sensors from carbon nanotubes self-assembled on aramid fibers, Journal of Intelligent Material Systems and Structures, (2014) 1-5.

[49] D.D. Chung, Self-monitoring structural materials, Materials Science and Engineering: R: Reports, 22 (1998) 57-78.

[50] R. Salvado, C. Lopes, L. Szojda, P. Araújo, M. Gorski, F.J. Velez, J. Castro-Gomes, R. Krzywon, Carbon Fiber Epoxy Composites for Both Strengthening and Health Monitoring of Structures, Sensors, 15 (2015) 10753-10770.